# Preamble Design Using Embedded Signalling for OFDM Broadcast Systems Based on Reduced-Complexity Distance Detection

Lifeng He, Zhaocheng Wang, *Senior Member, IEEE*, Fang Yang,
Sheng Chen, *Fellow, IEEE*, and Lajos Hanzo, *Fellow, IEEE*

***Abstract*— The second generation digital terrestrial television broadcasting standard (DVB-T2) adopts the so-called P1 symbol as the preamble for initial synchronization. The P1 symbol also carries a number of basic transmission parameters, including the fast Fourier transform size and the single-input/single-output as well as multiple-input/single-output mode, in order to appropriately configure the receiver for carrying out the subsequent processing. In this contribution, an improved preamble design is proposed, where a pair of training sequences is inserted in the frequency domain and their distance is used for transmission parameter signalling. At the receiver, only a low-complexity correlator is required for the detection of the signalling. Both the coarse carrier frequency offset and the signalling can be simultaneously estimated by detecting the above-mentioned correlation. Compared to the standardised P1 symbol, the proposed preamble design significantly reduces the complexity of the receiver while retaining high robustness in frequency-selective fading channels. Furthermore, we demonstrate that the proposed preamble design achieves a better signalling performance than the standardised P1 symbol, despite reducing the numbers of multiplications and additions by about 40% and 20%, respectively.**

***Index Terms*— Orthogonal frequency division multiplexing, second generation digital terrestrial television broadcasting standard, preamble, transmission parameter signalling**

## I. Introduction

Orthogonal frequency division multiplexing (OFDM) [1] has found its way into numerous recent standards operating in frequency-selective fading channels. With the aid of the inverse fast Fourier transform (IFFT) and fast Fourier transform (FFT) operations, both the modulation and demodulation operations of an OFDM system facilitate convenient hardware implementations. Hence, OFDM has been widely adopted in the areas of digital TV [2]–[5], wireless local area networks (WLANs) [1], [6] and in next generation mobile communications [7]–[9]. Multi-service broadcast has become an important research topic in both industry and academia. With the growing commercial demands for supporting multi-services, including HDTV, mobile TV and data-casting, broadcast systems are expected to provide a wide choice of transmission parameters in order to accommodate different quality of service (QoS) requirements. The European Telecommunications Standards Institute (ETSI) recently issued the second generation digital terrestrial television broadcasting standard (DVB-T2), which aims for providing multiple services in different propagation scenarios [5].

DVB-T2 [5] offers a total of six FFT sizes and seven diverse guard interval modes in order to adapt to different applications. Furthermore, both single-input/single-output (SISO) and multiple-input/single-output (MISO) transmission modes are supported. Therefore, the efficient and reliable detection of these basic system-configuration parameters is critical for the receiver to reliably perform its subsequent processing steps. For this reason, DVB-T2 adopts a specifically designed P1 symbol as the preamble of the DVB-T2 frame. Unlike conventional preambles, which are designed merely for supporting timing and frequency synchronization [10], [11], the P1 symbol also supports the basic transmission parameter signalling (TPS), including the FFT size and SISO/MISO mode [5]. In the time domain (TD), a novel cyclic extension structure is adopted in order to improve the peak of the guard interval correlation (GIC) for the sake of improved timing synchronization [12]. In the frequency domain (FD), a length-384 sequence carrying 7-bit signalling is mapped to a distributed sub-carrier pattern. To transmit the 7-bit signalling, the standardised P1 symbol of DVB-T2 exploits two sets of orthogonal complementary sequences in order to represent the different signalling fields, which are known as S1 and S2, respectively. At the receiver, all possible sequences of both sets are correlated with the received signalling sequence to find a matched case. The need to perform such a large number of correlations, however, imposes a high computational complexity on the signalling detection.

In this contribution, an improved preamble design is proposed, which carries out the same signalling task as the standardised P1 symbol based preamble at a lower complexity. Specifically, unlike in the standardised P1 symbol, which incorporates different sequences to convey the signalling information, the proposed preamble inserts a pair of training sequences in the FD, and the signalling information is conveyed by the distance between the pair. At the receiver, only a single correlator is required to simultaneously estimate both



L. He, Z. Wang and F. Yang are with Tsinghua National Laboratory for Information Science and Technology (TNList), Tsinghua University, Beijing, P. R. China (E-mails: hlf04@mails.tsinghua.edu.cn zcwang@tsinghua.edu.cn fangyang@tsinghua.edu.cn).

S. Chen and L. Hanzo are with School of Electronics and Computer Science, University of Southampton, Southampton SO17 1BJ, U.K. (E-mails: sqc@ecs.soton.ac.uk lh@ecs.soton.ac.uk).

This work was supported in part by Tsinghua University Initiative Scientific Research Program 20091081280 and in part by Standardization Administration of the People's Republic of China (SAC) with AQSIQ Project 200910244.

the TPS and the coarse carrier frequency offset (CFO), therefore the complexity of the receiver is significantly reduced. Furthermore, our simulation results show that the proposed preamble design achieves a better signalling performance than the standardised P1 symbol based preamble of the DVB-T2 for transmission over frequency-selective fading channels.

The rest of this contribution is organized as follows. Section II briefly describes the standardised P1 symbol in DVB-T2, while Section III provides the detailed design of the proposed preamble. Section IV presents our performance evaluation of the proposed preamble design through both theoretical analysis and computer simulation. The computational requirements of detecting both preambles are also compared in this section. Finally, our conclusions are summarized in Section V.

## II. P1 Symbol in DVB-T2

In this section, we commence with the signal model of OFDM systems and then focus our attention on the P1 symbol design of the DVB-T2 system.

### A. Signal Model

The transmitted TD signal of an OFDM system can be represented as

$$x_n = \frac{1}{\sqrt{N}} \sum_{k=0}^{N-1} X_k e^{j\frac{2\pi}{N}nk}, \tag{1}$$

where $N$ is the number of sub-carriers, and $X_k$ are the transmitted FD data symbols. The received TD OFDM symbol is represented by

$$y_n = x_{n-n_0} \otimes h_n e^{j2\pi f_c n} + \nu_n, \tag{2}$$

where the operator $\otimes$ denotes linear convolution, $n_0$ and $f_c$ denote the time delay and CFO, respectively, while $h_n$ and $\nu_n$ denote the channel impulse response (CIR) and the additive white Gaussian noise (AWGN), respectively. The channel's signal-to-noise ratio (SNR) is defined by $\rho = \sigma_s^2/\sigma_n^2$, where $\sigma_s^2 = E[|x_n|^2]$ is the signal power and $\sigma_n^2 = E[|\nu_n|^2]$ is the AWGN power, with $E[\bullet]$ denoting the statistical expectation operator.

OFDM systems are known to be sensitive to the CFO, which may be separated into two parts as follows

$$f_c = m_{\text{int}} \cdot \frac{1}{N} + f_{\text{frc}}, \tag{3}$$

where $\frac{1}{N}$ is the sub-carrier spacing, $m_{\text{int}}$ is an integer and $f_{\text{frc}}$ is the fractional part of the CFO, which is restricted in a range of

$$-\frac{1}{2N} < f_{\text{frc}} \leq \frac{1}{2N}. \tag{4}$$

The integer part of the CFO will lead to a cyclic shift in the FD, while the fractional CFO will impose inter-carrier interference (ICI), which may severely degrade the attainable performance [13]. In OFDM systems, the training symbols are often transmitted before the data blocks as preambles. The task of the preamble is to accomplish both timing and frequency synchronization as well as to detect the TPS, if it is present.

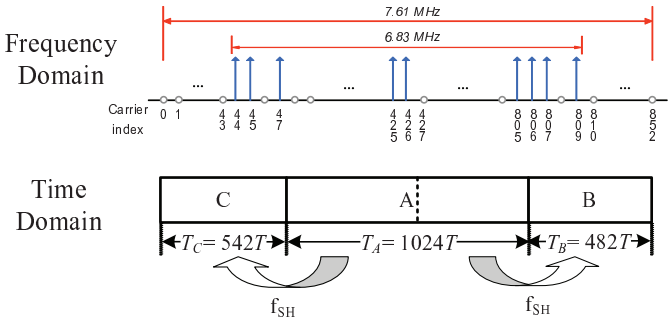


Fig. 1. Structure of the P1 symbol in DVB-T2.

### B. The standardised P1 Symbol

The P1 symbol defined in the DVB-T2 standard [5] is composed of a 1K OFDM symbol 'A' and its two cyclic extensions, which are denoted as 'C' and 'B', respectively. The C-A-B structure of the P1 symbol is illustrated in Fig. 1. The TD baseband signal of the P1 symbol is defined by

$$x_n = \begin{cases} p_A(n)e^{j2\pi f_{\text{SH}} n}, & 0 \leq n < 542, \\ p_A(n-542), & 542 \leq n < 1566, \\ p_A(n-1024)e^{j2\pi f_{\text{SH}} n}, & 1566 \leq n < 2048, \end{cases} \tag{5}$$

where $p_A(n)$ is the baseband representation of part 'A', $f_{\text{SH}}$ is the additional frequency shift applied to both parts 'B' and 'C' in order to distinguish the P1 symbol from the common cyclic prefix (CP) of the OFDM symbols.

Out of the 853 useful FD sub-carriers of the 1K symbol in 'A', only 384 sub-carriers are used, while the others are set to zero. The sub-carrier distribution of the P1 symbol is also illustrated in Fig. 1. The active carriers occupy roughly 6.83 MHz in the middle of the nominal 7.61 MHz bandwidth. Even a frequency shift of up to 500 kHz may be estimated, since most of the useful sub-carriers are still within the bandwidth. Therefore, the P1 symbol is robust to large CFOs.

The embedded P1 signalling contains two fields, referred to as the 3-bit signalling S1 and the 4-bit signalling S2, respectively. Specifically, the 3-bit S1 is represented by one of the 8 orthogonal complementary sequences of length 64, while the 4-bit S2 is represented by one of the 16 orthogonal complementary sequences of length 256 [5]. The S1 sequence, the S2 sequence and a repetition of the S1 sequence are concatenated to compose a length-384 signalling sequence, which is firstly differentially binary phase-shift keying (DBPSK) modulated, then scrambled, and finally mapped to the active sub-carriers. It should be noted that a total of $8 \times 16 = 128$ different signalling sequences correspond to the 7-bit signalling.

### C. Detection of the P1 Symbol

At the receiver, both timing and fractional CFO estimation may be achieved by the modified GIC method based on the C-A-B structure [12]. After the fractional CFO is compensated, part 'A' of the P1 symbol is extracted and transformed to the FD for integer CFO estimation and signalling detection. First, the energy-detection based sub-carrier pattern matching is performed to locate the exact positions of the active sub-carriers by correlating the received signal with the expected

carrier-distribution sequence (CDS) [14]. The CDS was specifically designed to ensure that only a perfect match gives a sufficiently high power correlation peak. The position of the correlation peak also gives an estimate of the integer part of the CFO, which is inferred from the peak's shift from its original position.

Once the active sub-carriers were identified, the receiver is ready to detect the S1 and S2 signalling. The length-384 signalling sequence is firstly extracted from the active carriers, then descrambled and differentially decoded. Finally, the 3-bit S1 and 4-bit S2 segments are separated from the signalling sequence. Each legitimate sequence of the S1 set is correlated with the received S1 signalling sequence one by one, and the sequence with the largest correlation peak is used for decoding the S1 signalling. Similarly, each legitimate sequence of the S2 set is correlated with the received S2 signalling sequence one by one to decode the S2 signalling. Since there are total of 8 sequences in the S1 set and 16 sequences in the S2 set, a large number of correlations are required. To reduce the complexity of computing such a large number of correlations, DVB-T2 adopted a series of complementary sets of sequences (CSS) [15]. These correlations may be determined with the aid of efficient correlators specifically designed for CSS [16]. However, the total computational complexity of the signalling detection remains high due to the specific design of the P1 symbol, which will be further discussed in Section IV.

## III. Design of the Proposed Preamble

In this section, we propose an improved preamble relying on a different signalling design, which is significantly less complex to decode.

### A. Structure of the Proposed Preamble

The structure of the proposed preamble is shown in Fig. 2, which inherits the structure of the standardised P1 symbol in the TD, while in the FD, the TPS design is different from that of the P1 symbol. Specifically, a pair of FD training sequences, denoted by $(a, b)$, are inserted into the sub-carriers. The FD values $\{X_k\}_{k=0}^{N-1}$ of part 'A' in the proposed preamble are represented by

$$X_k = \begin{cases} a_{k-512+\lfloor \frac{\Delta L}{2} \rfloor + L}, & 512 - L - \lfloor \frac{\Delta L}{2} \rfloor \le k < 512 - \lfloor \frac{\Delta L}{2} \rfloor, \\ b_{k-512-\lceil \frac{\Delta L}{2} \rceil}, & 512 + \lceil \frac{\Delta L}{2} \rceil \le k < 512 + L + \lceil \frac{\Delta L}{2} \rceil, \\ 0, & \text{others}, \end{cases} \quad (6)$$

where $\lceil \bullet \rceil$ and $\lfloor \bullet \rfloor$ denote the integer ceiling and floor operators, respectively, $L$ is the length of $a$ and $b$, while $\Delta L$ denotes the FD distance between $a$ and $b$, which varies according to the TPS requirements. The FD sub-carrier symbols $\{X_k\}_{k=0}^{N-1}$ are then converted to the TD to create part 'A' of the TD preamble by the $N$-point IFFT, as defined in (1).

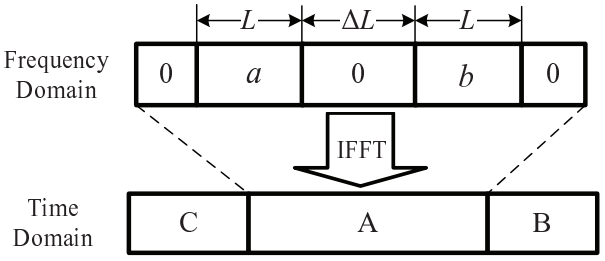


Fig. 2. Structure of the proposed preamble.

The proposed preamble varies the distance between the pair of FD training sequences to create a signalling regime, where the FD distance may be varied across a wide range of values to satisfy the requirement of conveying 7-bit signalling. Taking a pair of length-255 training sequences, for example, the pair occupies two consecutive 255 sub-carrier segments, which are allocated symmetrically from the centre of the nominal bandwidth, as seen in Fig. 2. The value of $\Delta L$ is chosen to vary in the range of $[128, 255]$ so that the required 7-bit signalling can be encoded into the 128 legitimate distance values. Further referring to the FD part of Fig. 2, the sub-carriers at the both ends are reserved so that the preamble can cope with large CFOs. The sub-carriers in the centre of the bandwidth are also reserved in order to reduce the impact of carrier leakage.

The performance associated with the proposed preamble depends on the chosen pair of FD training sequences. There are three main considerations in choosing these two training sequences: good auto-correlation property, simple correlator implementation, and low peak-to-average power ratio (PAPR) in the TD after the IFFT operation. Pseudo-noise (PN) sequences are widely used as training sequences since they have beneficial correlation properties. The optimal PN sequence may be found by searching through the entire PN sequence set [17] in order to ensure the lowest PAPR for the TD preamble. We suggest the pair $(a, b)$ to be the pair of identical DBPSK modulated PN sequences, which have the lowest PAPR in the TD after the IFFT operation.

### B. Detection of the Proposed Preamble

In the receiver, the GIC method of [12] is applied for timing and fractional CFO estimation. Afterwards, the TD part 'A' is extracted from the preamble and converted to the FD by the $N$-point FFT operation, yielding

$$Y_k = \frac{1}{\sqrt{N}} \sum_{n=0}^{N-1} \left( y_n e^{-j2\pi \hat{f}_{\text{frc}} n} \right) e^{-j\frac{2\pi}{N}nk}, \ 0 \le k < N, \quad (7)$$

where $\hat{f}_{\text{frc}}$ is the estimated fractional CFO, which is compensated in the TD before the FFT operation. The FFT result $\{Y_k\}_{k=0}^{N-1}$ is firstly differentially detected in the FD, i.e. $Y_k \cdot Y_{k-1}^*$, and then correlated with the local PN sequence $\{C_k\}_{k=0}^{L-1}$ to yield

$$R_l = \frac{\sum_{k=0}^{L-1} \left( Y_{l+k} \cdot Y_{l+k-1}^* \right) \cdot C_k}{\frac{1}{2} \sum_{k=0}^{N-1} |Y_k|^2}, \ 0 \le l < N - L, \quad (8)$$

where $C_k$ is the sequence assigned to $a$ and $b$ before DBPSK modulation, while $^*$ denotes the complex conjugation. Since $\{C_k\}$ is a binary sequence, which assumes values from the set $\{-1, +1\}$, the multiplications by $C_k$ in the correlation (8) may be realised by a series of adders instead of multipliers. This

significantly reduces the complexity of the proposed signalling detection algorithm.

Since there are two identical training sequences in $\{Y_k\}$, two peaks are expected in the correlation result in (8), and the distance between the two peaks gives an estimate of $\Delta L$ as

$$\Delta\hat{L} = k_2 - k_1 - L, \tag{9}$$

where $k_1$ and $k_2$ are the correlation peak positions in the first and second half of $\{R_k\}$, respectively, namely,

$$k_1 = \arg \max_{0 \le l < \frac{N}{2}} |R_l|, \tag{10}$$

$$k_2 = \arg \max_{\frac{N}{2} \le l < N} |R_l|. \tag{11}$$

The $\Delta\hat{L}$ value of (9) is then used to decode the 7-bit signalling information. The two peak positions also yield an estimate of the integer CFO, which is inferred from the peaks' shifts with their designed positions according to

$$\hat{m}_{\text{int}} = \begin{cases} k_1 - \left(512 - \left\lfloor \frac{\Delta L + L}{2} \right\rfloor\right), & \text{if } |R_{k_1}| \ge |R_{k_2}|, \\ k_2 - \left(512 + \left\lceil \frac{\Delta L + L}{2} \right\rceil\right), & \text{if } |R_{k_1}| < |R_{k_2}|. \end{cases} \tag{12}$$

In contrast to the standardised P1 symbol, which requires a large number of correlations at the receiver for detecting the TPS, the proposed preamble design only requires a single correlator for detecting the TPS, hence yielding a considerable reduction in the receiver's complexity.

An example of the correlation function of (8) recorded for transmission over the AWGN channel at SNR $= 0$ dB is shown in Fig. 3. We observe a shift of the correlation peak for CFO $=$ 500 kHz from the reference position of CFO $= 0$. This shift gives a fine estimate of the integer CFO. It can also be seen from Fig. 3 that an accurate estimate of $\Delta L$ may be inferred from the distance between the two correlation peaks.

## IV. Performance Evaluation

We first analyse the theoretical performance of the proposed preamble design in the AWGN channel, and then compare its signalling performance for transmission over frequency-selective fading channels to that of the standardised P1 preamble using simulations. A comparison of the signalling detection complexity required by the two designs is also given.

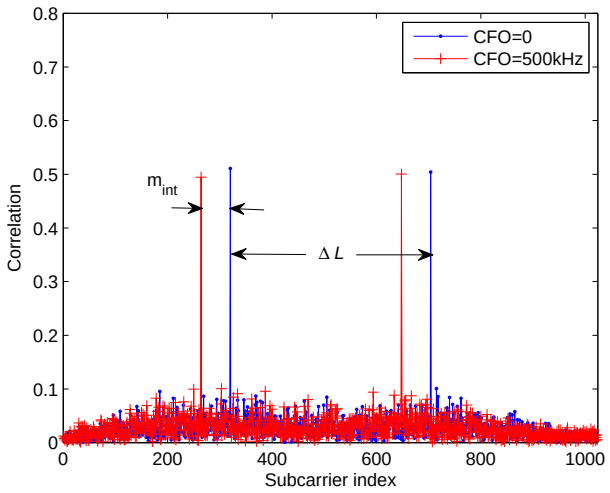


Fig. 3. Correlation results of the proposed preamble design in the AWGN channel given SNR=0 dB.

### A. Theoretical Lower Bound over AWGN Channel

Assuming an ideal fraction CFO compensation in (7), the correlation peaks can be approximated by $R_{k_1} = X_R + \tilde{V}_{k_1}$ and $R_{k_2} = X_R + \tilde{V}_{k_2}$, where $X_R$ is real-valued, while $\tilde{V}_{k_1}$ and $\tilde{V}_{k_2}$ are complex-valued zero-mean random variables. Following a similar approach to the one given in [10], we can conclude that the real and imaginary parts of both $R_{k_1}$ and $R_{k_2}$ have the Gaussian distributions $N(\mu_R, \sigma_R^2)$ and $N(0, \sigma_R^2)$, respectively, where $\mu_R$ and $\sigma_R^2$ are given by [10]

$$\mu_R = \frac{\rho}{\rho + 1}, \tag{13}$$

$$\sigma_R^2 = \frac{(1 + \mu_R^2)\rho + (2L/N + \mu_R^2)}{N(\rho + 1)^2}. \tag{14}$$

Hence, the peak metrics $|R_{k_1}|$ and $|R_{k_2}|$ follow the same Rician distribution given by

$$f_{\text{peak}}(y) = \frac{y}{\sigma_R^2} e^{-\frac{y^2 + \mu_R^2}{2\sigma_R^2}} I_0\left(\frac{\mu_R \cdot y}{\sigma_R^2}\right), \; y > 0, \tag{15}$$

where $I_0(\bullet)$ is the zero-order modified Bessel function of the first kind [18].

Assuming that the correlation of the training sequences is unity for a perfect alignment and zero otherwise, both the real and imaginary parts of the side-lobes follow the Gaussian distribution $N(0, \sigma_R^2)$. Thus, the side-lobe metric $|R_k|_{k \ne k_1, k_2}$ has a Rayleigh distribution given by

$$f_{\text{side}}(y) = \frac{y}{\sigma_R^2} e^{-\frac{y^2}{2\sigma_R^2}}, \; y > 0. \tag{16}$$

The expectations of the correlation peak and side-lobes at different SNRs are illustrated in Fig. 4, where the dashed lines indicate the standard deviations from the expectation. We can observe that for SNR$\ge -5$ dB, the correlation metric can reliably separate the peak and the side-lobes.

Next the probability of false detection is analysed. Considering the first half of $\{R_k\}$, the probability that the side-lobe

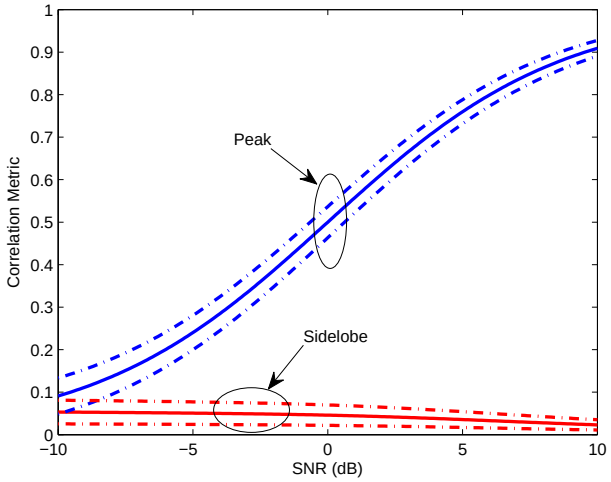


Fig. 4. Expectations of the correlation metric for the proposed preamble design in the AWGN channel given different SNR values, where the dashed lines indicate the standard deviations from the expectation.

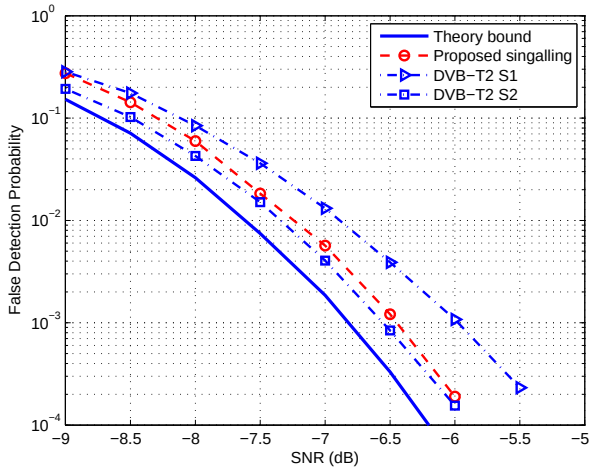


Fig. 5. False detection probabilities of the proposed signalling as well as the DVB-T2 S1 and S2 signalling over the AWGN channel, in comparison with the theoretical bound.

$|R_k|_{k\neq k_1}$ is higher than $|R_{k_1}|$ is given by

$$P\left(|R_k|_{k\neq k_1} > |R_{k_1}|\right) = \int_0^{+\infty} \frac{y}{\sigma_R^2} e^{-\frac{2y^2+\mu_R^2}{2\sigma_R^2}} I_0\left(\frac{\mu_R \cdot y}{\sigma_R^2}\right) dy. \tag{17}$$

The false peak detection probability is thus

$$\begin{aligned} P_f &= P\Big(\Big\{ \max_{0\leq k<\frac{N}{2}, k\neq k_1} |R_k| \Big\} > |R_{k_1}| \Big) \\ &= 1 - \Big(1 - P\left(|R_k|_{k\neq k_1} > |R_{k_1}|\right)\Big)^{\frac{N}{2}-1}. \end{aligned} \tag{18}$$

If the both correlation peaks are detected, the estimation of $\Delta L$ and $m_{\rm int}$ is deemed to be achieved. Thus the false detection probability for $\Delta L$, denoted as $P_{{\rm FD},\Delta L}$, and the false detection probability for $m_{\rm int}$, denoted as $P_{{\rm FD},m_{\rm int}}$, are given by

$$P_{{\rm FD},\Delta L} = P_{{\rm FD},m_{\rm int}} = 1 - (1 - P_f)^2, \tag{19}$$

both of which are a function of the SNR.

The theoretical lower bound (19) is depicted in Fig. 5, in comparison to the performance of the proposed signalling detection obtained by simulation, which exhibited about 0.4 dB degradation from the theoretical bound. The degradation of the actual signalling detection from the theoretical lower bound is mainly due to the following two factors. Firstly, having a realistic timing recovery imposes some phase rotation after the FFT based demodulation. Secondly, the residual fractional CFO imposes some ICI, which also results in an SNR loss, quantified as [13]

$$\text{SNR}_{\rm loss}\ \text{(dB)}\ \leq 10 \cdot \log\left(\frac{1 + 0.5947 \cdot \text{SNR} \cdot (\sin \pi\varepsilon)^2}{(\sin \pi\varepsilon/\pi\varepsilon)^2}\right), \tag{20}$$

where $\varepsilon = f_{\rm frc} - \hat{f}_{\rm frc}$ is the normalised residual CFO after the fractional CFO compensation.

The signalling detection performance of the standardised P1 symbol over the AWGN channel obtained by simulation is also given in Fig. 5 for comparison. Note that the S1 and S2 fields of the standardised P1 symbol have different priorities while the 7-bit signalling of the proposed preamble has the same priority. It can be seen from Fig. 5 that the detection performance of the S2 signalling is marginally better than that of the proposed preamble, while the detection performance of the proposed signalling is much better than that of the S1 signalling. Thus, the signalling detection performance of the proposed preamble design is better than the average signalling detection performance of the standardised P1 symbol over the AWGN channel.

### *B. Simulations over Frequency-Selective Channels*

A simulation study was then carried out to compare the signalling detection performance of the proposed preamble with that of the standardised P1 symbol for transmission over frequency-selective channels. The same DVB-T2 transmission parameters were adopted and the signal powers of both preambles were normalised in the simulation to ensure a fair comparison. The duration of the both preambles was 224 $\mu s$ in the nominal 8 MHz system. The Brazil DTV field testing 2nd channel model (Brazil-B) [4] and the China DTV testing 8th channel model (CDT-8) [19] were adopted in the simulation. It should be noted that an unattenuated echo occurs in the CDT-8 channel at a delay of 30 $\mu$s, which results in severe frequency selectivity. The signalling error rate (SER), defined as the false signalling detection probability, was evaluated.

Fig. 6 depicts the SER results obtained for the S1 and S2 signalling of the P1 preamble as well as for the proposed signalling (labelled as Sp) over the Brazil-B and CDT-8 static channels, while Fig. 7 compares the results for the Brazil-B and CDT-8 fading channels with 50 Hz Doppler frequency. For the Brazil-B channel whose frequency selectivity is not severe, it can be observed that the proposed signalling achieved a similar SER as the S2 signalling, while outperforming the S1 signalling. It can also be seen from Figs. 6 and 7 that the proposed signalling achieved the performance gains by about 2.5 and 1.5 dB, respectively, at the SER level of $10^{-2}$ over the severely frequency-selective CDT-8 static and fading channels. The reason for much better signalling performance of the proposed preamble for transmission over severely frequency-selective channels can be explained as follows. Both the

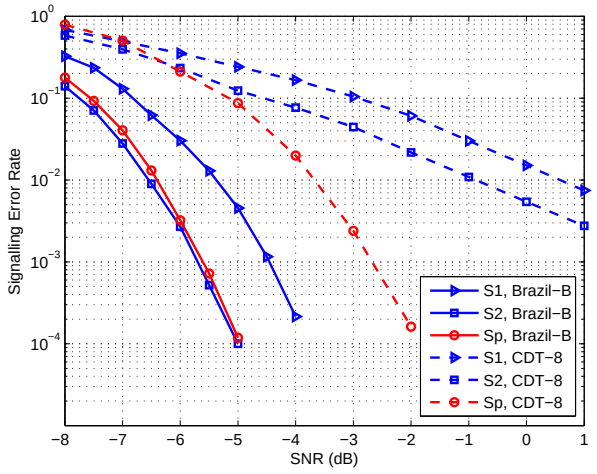


Fig. 6. Signalling error rate comparison of the S1 and S2 signalling in the P1 preamble as well as the proposed signalling (Sp) over the Brazil-B and CDT-8 frequency-selective static channels.

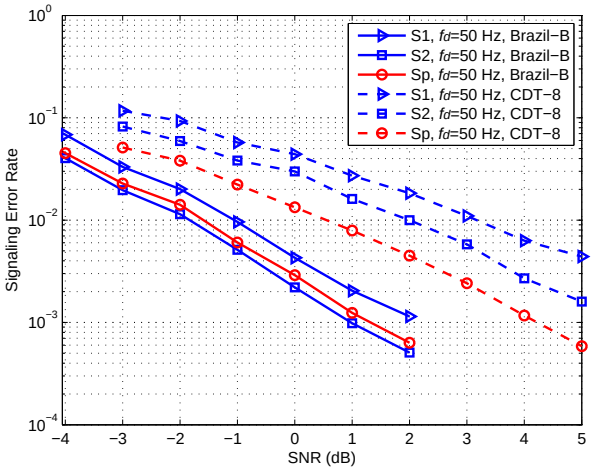


Fig. 7. Signalling error rate comparison of the S1 and S2 signalling in the P1 preamble as well as the proposed signalling (Sp) over the Brazil-B and CDT-8 frequency-selective fading channels with 50 Hz Doppler frequency.

P1 symbol and proposed design use differential decoding to alleviate the impact of the channel phase. The larger the phase difference for two adjacent sub-carriers is, the less effective this differential decoding is. The frequency response of the CDT-8 channel varies significantly from sub-carrier to sub-carrier owing to the severe channel frequency selectivity. The active sub-carriers in the standardised P1 symbol are randomly distributed in the FD, and the phases of two adjacent active sub-carriers can differ significantly. By contrast, the phase difference of two adjacent sub-carriers is much smaller for the proposed preamble, whose sub-carriers are closely adjacent.

### C. Comparison of Computational Complexity

As detailed in Section II, the detection of the P1 signalling in DVB-T2 includes four main steps: the sub-carrier pattern matching, descrambling, differential detection and correlation with the local CSS. By contrast, the proposed detection of the 7-bit signalling information only requires differential decoding and correlation with the local PN sequence. The computational complexity of the signalling detection algorithm may be quantified in terms of the number of multiplications and additions required. Assuming that the system is designed to cope with a maximum CFO of $\pm 500$ kHz, i.e., up to $\pm 56$ sub-carriers, the total number of computations imposed by detecting the standardised P1 signalling includes

$$\begin{aligned} &384 + 56 \times 2 + 384 \times 2 = 1,264 \\ &\quad \text{[complex-valued multiplications]} \\ &384 \times 56 \times 2 + 256 + 128 + 64 \times 48 = 78,848 \\ &\quad \text{[complex-valued additions].} \end{aligned} \tag{21}$$

By contrast, the proposed signalling detection requires

$$\begin{aligned} &255 \times 2 + 56 \times 2 + 128 = 750 \\ &\quad \text{[complex-valued multiplications]} \\ &255 \times (56 \times 2 + 128) = 61,200 \\ &\quad \text{[complex-valued additions].} \end{aligned} \tag{22}$$

The proposed signalling detection method reduces the number of multiplications by about 40% and the number of additions by 20%, in comparison to the standardised P1 symbol design.

## V. Conclusions

An improved preamble has been designed for signalling in OFDM broadcast systems, which exploits the presence of 128 possible distances between a pair of training sequences in the FD to infer the 7-bit signalling information. Only a single correlator is required at the receiver for signalling detection. Compared to the standardised P1 symbol of DVB-T2, the proposed design reduces the numbers of multiplications and additions by about 40% and 20%, respectively. The simulation results have also shown that the proposed preamble achieves a better signalling detection performance, in terms of false detection probability, than the standardised P1 preamble.

## References

[1] L. Hanzo, M Münster, B. J. Choi and T. Keller, *OFDM and MC-CDMA for Broadband Multi-User Communications, WLANs and Broadcasting*. Chichester, U.K.: John Wiley & Sons, 2003.

[2] H. Sari and G. Karam, "Orthogonal frequency division multiple access and its application to CATV networks," *Eur. Trans. Commun.*, vol. 45, pp. 507–516, Nov. 1998.

[3] M. Takada and M. Saito, "Transmission system for ISDB-T," *Proc. IEEE*, vol. 96, no. 1, pp. 251–256, Jan. 2006.

[4] J. Song, Z. X. Yang, L. Yang, K. Gong, C. Y. Pan, J. Wang and Y. S. Wu, "Technical review on Chinese digital terrestrial television broadcasting standard and measurements on some working modes," *IEEE Trans. Broadcast.*, vol. 53, no. 1, pp. 1–7, Mar. 2007.

[5] *Frame Structure Channel Coding and Modulation for a Second Generation Digital Terrestrial Television Broadcasting System (DVB-T2)*. DVB Document A122, ETSI Std., Jun. 2008.

[6] *IEEE Standard for Wireless LAN Medium Access Control (MAC) and Physical Layer (PHY) Specifications*. IEEE 802.11, Nov. 1997.

[7] H. Ekstrom, A. Furuskar, J. Karlsson, M. Meyer, S. Parkvall, J. Torsner, and M. Wahlquist, "Technical solutions for the 3G long-term evolution," *IEEE Commun. Mag.*, vol. 44, no. 3, pp. 38–45, Mar. 2006.

[8] *IEEE Standard for Local and Metropolitan Area Networks. Part 16: Air Interface for Fixed and Mobile Broadband Wireless Access Systems*. IEEE 802.16e, Feb. 2006.

[9] F. Khan, *LTE for 4G Mobile Broadband: Air Interface Technologies and Performance*. Cambridge, U.K.: Cambridge University Press, 2009.

[10] T. M. Schmidl and D. C. Cox, "Robust frequency and timing synchronization for OFDM," *IEEE Trans. Commun.*, vol. 45, no. 12, pp. 1613–1621, Dec. 1997.

[11] F. Tufvesson, M. Faulkner, and O. Edfors, "Time and frequency synchronization for OFDM using PN sequence preambles," in *Proc. VTC'99-Fall*, Sep. 1999, vol. 4, pp. 2203–2207.

[12] J. G. Doblado, V. Baena, A. C. Oria, D. Perez-Calderon, and P. Lopez, "Coarse time synchronisation for DVB-T2," *Electron. Lett.*, vol. 46, no. 11, pp. 797–799, May 2010.

[13] P. H. Moose, "A technique for orthogonal frequency division multiplexing frequency offset correction," *IEEE Trans. Commun.*, vol. 42, no. 10, pp. 2908–2914, Oct. 1994.

[14] *Implementation Guidelines for a Second Generation Digital Terrestrial Television Broadcasting System (DVB-T2)*. DVB Document A133, ETSI Std., Feb. 2009.

[15] C. C. Tseng, and C. L. Liu, "Complementary sets of sequences," *IEEE Trans. Inform. Theory*, vol. IT-18, no. 5, pp. 644–652, Sep. 1972.

[16] C. D. Marziani, J. Urena, A. Hernandez, M. Mazo, F. J. Alvarez, J. J. Garcia, P. Donato, "Modular architecture for efficient generation and correlation of complementary set of sequences," *IEEE Trans. Signal Processing*, vol. 55, no. 2, pp. 2323–2337, May 2007.

[17] T. May, H. Rohling, and O. Edfors, "Reducing the peak-to-average power ratio in OFDM radio transmission systems," in *Proc. VTC'98-Spring*, May 1998, vol. 3, pp. 2474–2478.

[18] H. G. Proakis, *Digital Communications* (Third edition). McGraw-Hill Book Co., 1995.

[19] F. Yang, J. T. Wang, J. Wang, J. Song, and Z. X. Yang, "Novel channel estimation method based on PN sequence reconstruction for Chinese DTTB system," *IEEE Trans. Consum. Electron.*, vol. 54, no. 4, pp. 1583–1589, Nov. 2008.